



Contents lists available at ScienceDirect



Catalysis Today

journal homepage: www.elsevier.com/locate/cattod

Direct synthesis of H₂O₂ over Pd supported on rare earths promoted zirconia

A. Bernardini^a, N. Gemo^b, P. Biasi^{b,c,*}, P. Canu^a, J.P. Mikkola^{b,c}, T. Salmi^b, R. Lanza^d

^a Università degli Studi di Padova, Dipartimento di Ingegneria Industriale, Via Marzolo n. 9, 35131 Padova, Italy

^b Åbo Akademi University, Laboratory of Industrial Chemistry and Reaction Engineering, Process Chemistry Centre, Åbo Akademi University, Biskopsgatan 8, 20500 Turku/Åbo, Finland

^c Umeå University, Department of Chemistry, Chemical-Biochemical Centre (KBC), Technical Chemistry, Umeå University, SE-90187 Umeå, Sweden

^d KTH—Royal Institute of Technology, Department of Chemical Engineering and Technology, Chemical Technology, SE-100 44 Stockholm, Sweden

ARTICLE INFO

Article history:

Received 13 October 2014

Received in revised form

11 December 2014

Accepted 15 December 2014

Available online xxxx

In memory of the Charismatic Professor Benedetto Corain (July 8th 1941–September 24th 2014), a catalyst for our research activities and ideas.

Keywords:

Palladium

H₂O₂ direct synthesis

Zirconia

Ceria

Rare earths

ABSTRACT

In this work Pd (0.3 or 0.6 wt.%) was supported on both Zr_xM_{1-x}O₂ (M = La, Y, Ce) and on mechanical mixtures of CeO₂ and ZrO₂. The synthesized catalysts were characterized by XRD, TPR, AAS and CO chemisorption and tested for the direct synthesis of hydrogen peroxide in a high pressure semibatch apparatus. The reactants conversion was limited in order to avoid mass-transfer limitations. No selectivity enhancers of any kind were used and all the materials were halide free. Small metal particles were obtained (1–2.6 nm). Supports with smaller pore diameters led to larger Pd particles, which in turn were found to preferentially support the formation of the peroxide. Moreover, supports with higher reducibility favored the production of H₂O₂, probably due to an easier reduction of the active metal, essential to achieve high selectivity. Notwithstanding the absence of enhancers, the specific activity and selectivity recorded were very high.

© 2015 Elsevier B.V. All rights reserved.

1. Introduction

Hydrogen peroxide is considered one of the most environmentally friendly and efficient oxidizing agents available to the industry. Its direct production from H₂ and O₂ (direct synthesis, DS) has been attracting considerable interest because of the potentially reduced costs and flexibility of the process [1,2]. Although the DS is in principle the simplest route to the peroxide, the reactions involve multiple consecutive and parallel paths leading to water (**Scheme 1**), which is by far thermodynamically favored. This adversely affects the selectivity and limits the yield of H₂O₂.

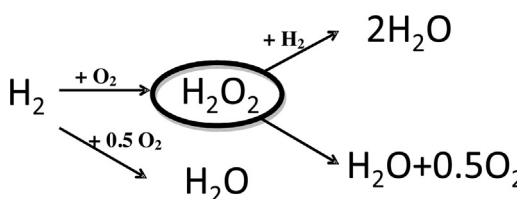
Therefore, the selectivity towards H₂O₂ is the first issue for a viable industrial application. Many Authors investigated the reaction conditions, trying to suppress the undesired side reactions [1–4]. The hydrogenation of hydrogen peroxide appears the major

consumption route of the peroxide produced [5–7]. The direct synthesis of water also contributes to impair the selectivity [5]. Catalyst design is the main tool to improve the selective synthesis of H₂O₂. Researchers investigated the catalyst properties to limit the undesired side reactions [1,2]. Pd has proven to be the best active metal, also on standard supports such as carbon, SiO₂ or Al₂O₃. Mineral acids and halides (either Cl⁻ or Br⁻) are known to be effective selectivity enhancers [1,2], especially in conjunction, but corrosion and metal leaching could become relevant issues. In addition, halide ions can be detrimental in down-stream applications.

Catalytic supports are known to play an important role in the selectivity towards the peroxide because of the interaction with the active metal. Hutchings et al. stated that the major parameter to favor the peroxide formation is a low isoelectric point, so that C was favored upon Al₂O₃, TiO₂ and MgO [8]. Acidic supports were found very promising also in others studies, specifically depositing Pd on a mesoporous ion exchange resin functionalized with sulfonic groups [9,10]. More recently, Abate et al. [11,12] investigated Pd supported on SiO₂, SBA15-15, γ-Al₂O₃ and N-CNT and found no apparent relationship between reactivity and selectivity and the acidity of the support, concluding that their data better

* Corresponding author at: Åbo Akademi University, Department of Chemical Engineering, Laboratory of Industrial Chemistry, Biskopsgatan 8, 20500 Turku/Åbo, Finland. Tel.: +358 22154555.

E-mail address: bpierdom@abo.fi (P. Biasi).

**Scheme 1.** Reactions involved in the direct synthesis of H_2O_2 .

correlated with the metal particle size [11]. Pd-based catalysts supported on silica were also successfully tested by Strukul et al. [13]. In their work, the authors concluded that SBA-15 was the most suitable support due to its ability to give the ideal Pd dispersion. Menegazzo et al. [14,15] compared Pd and Pd-Au catalysts over SiO_2 , ZrO_2 , $\text{ZrO}_2/\text{SO}_4^-$, CeO_2 , $\text{CeO}_2/\text{SO}_4^-$, confirming that Pd/ SiO_2 gave the highest selectivity [14]. The authors also proposed that a lower selectivity was achieved with the other supports because of the smaller Pd particles formed, preferentially leading to the formation of water [14,16]. It has also been shown that the reduced form of Pd is apparently more active and selective in the H_2O_2 direct synthesis [9,17], with Pd oxide been almost inactive [17].

Following these inspiring results, in this work we tried to investigate the relationship between the support properties, the deposition of the active metal phase and the activity and selectivity of the resulting catalysts. To the best of our knowledge, no studies have yet been done using ceria and zirconia mixtures and solutions ($\text{Zr}_x\text{Ce}_{1-x}\text{O}_2$) or zirconia stabilized with rare earths. These materials present unique features, such as increased dispersion [18] and O_2 mobility [19], which favors the active metal activity, especially in conditions in which the reducibility of the catalytic systems plays an important role [20]. Furthermore, the properties of these materials can be easily changed and adapted to specific applications. Indeed, their surface area, pore volume, particle size, homogeneity etc, can be tuned with different preparation procedures [21,22]. An increased metal-support interaction should also allow decreasing the metal loading, which would reduce the cost of the catalysts. We focused on Pd supported on mixed oxides (ZrO_2 and CeO_2) and rare earth elements (Y_2O_3 and La_2O_3) with different surface properties in order to access different particle size and metal dispersions. Both homogeneous solid solutions and mechanical mixtures of ZrO_2 with different promoters were tested. Catalysts prepared by incipient wetness impregnation were characterized by X-ray diffraction, temperature programmed reduction, CO chemisorption, atomic absorption spectroscopy and nitrogen adsorption analyses. Hydrogen peroxide direct synthesis was performed in a novel high pressure semibatch apparatus. Although they are known to favor the selectivity toward the peroxide, neither promoters nor stabilizers (halides and acids) were introduced in the reaction environment to focus on the support-Pd interaction solely. In order to avoid any traces of halides, all catalysts were prepared from halide free chemicals. The support properties were related to the structure of the active metal particles, which in turns was found to affect the activity and selectivity toward the peroxide.

2. Materials and methods

2.1. Catalyst preparation

Seven Pd catalyst samples were prepared by incipient wetness impregnation of different support powders. A 1 wt.% Pd on carbon commercial catalysts was purchased by Sigma Aldrich and used as received. Most of the supports were provided by MEL Chemicals, while others were obtained by mixing, crushing together and calcining ceria and zirconia powders supplied by Evonik and bought from Alfa Aesar, respectively. Palladium (II) nitrate hydrate 99.9%,

Table 1
List, composition and suppliers of the materials used.

Label	Support (wt.%)	Supplier	Product code/CAS
Pd2	$\text{ZrO}_2/\text{CeO}_2$ 82.5/17.5	MEL Chemicals	XZO 802
Pd3	Ce doped ZrO_2	MEL Chemicals	XZO
Pd4	$\text{ZrO}_2/\text{CeO}_2$ 50/50	Evonik/Alfa Aesar	0857
Pd5	$\text{ZrO}_2/\text{CeO}_2$ 17.5/82.5	Evonik/Alfa Aesar	
Pd6	$\text{ZrO}_2/\text{Y}_2\text{O}_3$ 92/8	MEL Chemicals	XZO 1012
Pd7	$\text{ZrO}_2/\text{CeO}_2/\text{La}_2\text{O}_3$ 77.5/17.5/5	MEL Chemicals	XZO 892
Pd8	CeO_2 ZrO_2	Evonik Alfa Aesar	VP AdNano® Ceria 50 1314-23-4

from Alfa Aesar, was used as metal precursor. The metal loading was 0.3 wt.% for the samples prepared using MEL Chemicals supports and 0.6 wt.% for the remaining ones. A higher metal loading was chosen for the latter samples to assure a high enough activity, since they are not expected to form a solid solution, which represents a more active support. All the support used, their composition and the catalyst prepared are listed in Table 1. About 8 g of each support were calcined in air atmosphere at 550 °C for 5 h, with a heating rate of 5 °C/min. The calcination conditions were chosen in order to assure the formation of a solid solution between ceria and zirconia. Indeed, according to MEL Chemicals, their supports form a solid solution upon calcination at 500–550 °C. The calcined supports were afterwards impregnated with a solution of $\text{Pd}(\text{NO}_3)_2$. The impregnation was done in 3 steps on samples 2, 4, 5 and 8, while the remaining supports needed 6 (sample 7) and 7 steps (samples 3 and 6), due to their low pore volume.

The surface area, pore volume and the pore average diameter of each support are reported in Table 2. The powders were dried at 90 °C in a ventilated oven for 2 h after each impregnation step. All the samples were calcined in air at 500 °C for 4 h, increasing the temperature at a rate of 5 °C/min. Finally, before the catalytic tests, all the catalysts were reduced in a furnace in pure H_2 flow (50 N ml/min) at 300 °C for 2 h, increasing the temperature at 5 °C/min in 50 N ml/min argon flow.

2.2. Catalyst characterization

The surface area and porosity analyses were performed with a Micromeritics ASAP 2000 unit. The samples were de-gassed by evacuation at 250 °C for a minimum of 4–5 h prior to analysis. Data were collected at liquid nitrogen boiling temperature (77 K). The surface area was calculated by the BET (Brunauer–Emmett–Teller) method with data collected at relative pressures between 0.06 and 0.2. The total pore volume was measured at p/p_0 of 0.99. The pore diameter distribution was determined using the BJH (Barrett–Joyner–Halenda) method.

X-ray diffraction patterns (XRD) were obtained using a Siemens D5000 diffractometer with a $\text{Cu K}\alpha$ monochromatic radiation, a scanning range 2θ between 10 and 90° and a step size of 0.02° and a time/step ratio of 1.0 s.

Temperature programmed reduction (TPR) tests were performed with a Micromeritics Autochem 2910 equipped with a TCD detector. The samples were flushed in helium at 250 °C for 2 h prior to analysis and cooled down to room temperature. The analysis was run using 5% H_2 in Ar up to 700 °C, with a heating rate of 5 °C/min.

The metal dispersion and average particle size were estimated by means of CO chemisorption, using a Micromeritics ASAP 2020 unit. The samples were evacuated in helium at 100 °C for 30 min, then at 350 °C for 15 min. After the evacuation, the powder was reduced with H_2 at 350 °C for 2 h. The analysis was performed dosing CO at 35 °C, assuming a CO/Pd stoichiometric ratio of 1, after a further evacuation step.

The samples metal loading was measured by atomic absorption spectroscopy (AAS) with a Perkin Elmer 1100 B equipped with a

Table 2

Surface features of the supports used.

Sample	BET area (m^2/g) [*]	Pore volume (cm^3/g) [*]	Pore Ø (nm) [*]	AAS metal loading (%)	Dispersion (%)	Particle size (nm)	Metal surf. area ($\text{m}^2/\text{g}_{\text{metal}}$)
Pd2	51.7	0.216	16.7	0.29	48.5	2.3	216
Pd3	93.4	0.115	4.9	0.34	55.6	2.0	248
Pd4	31.4	0.198	25.2	0.66	61.9	1.8	276
Pd5	44.2	0.310	28.0	0.62	80.7	1.4	359
Pd6	71.6	0.125	7.0	0.26	52.5	2.1	234
Pd7	102.0	0.118	4.7	0.30	42.4	2.6	189
Pd8	71.3	0.290	16.3	0.54	99.1	1.1	441

^{*} Bare support.

Pd Lumina Hollow Cathode Lamp. 20 mg of dried sample were dissolved in an aqua regia solution and then diluted with deionized water.

2.3. Reactor set up

The catalysts were tested in a slurry methanol solution, within a 300 ml autoclave operated in semibatch mode. A schematic of the apparatus is given in Fig. 1.

Methanol (200 ml) was introduced in the reactor first, followed by the gas reagents. Throughout the experiments, the gas mixture was continuously bubbled into the static liquid phase by a gas diffuser via 3 mass flow controllers. The gas composition was 76.5–20–3.5 mol% N_2 – O_2 – H_2 , respectively, with a total flow of 300 N ml/min. Before the introduction of the catalyst, the temperature was decreased at 10 °C and stirring started (1000 rpm), allowing the pressure to reach the desired value (50 bar). Pressure inside the reactor was kept constant via a back pressure controller. The gas composition at the outlet was measured by gas chromatography analysis to ensure the vapor–liquid equilibrium was reached before the test was initiated. Last, the catalyst (60 mg) was introduced via a dedicated chamber. The reactions were assumed to start as the catalyst was lead into the reactor. Note that introducing the catalyst last ensured no in situ oxidation/reduction of the catalyst due to a potential contact with the reagents before the beginning of the experiment. Moreover, this procedure allows for a very precise identification of the beginning of the reactions. Liquid samples were collected at increasing time up to 5 h via a sampling valve. The gas outlet was equipped with a condenser (operating at –18 °C) to ensure that no methanol left the reactor with the outgoing gas flow. The efficiency of the condenser was verified by gas chromatography analysis, and no methanol was detected in the gas flow leaving the system.

H_2O_2 and H_2O concentrations were determined by iodometric and Karl-Fischer titrations, respectively. The measured

concentrations were rescaled on the moles of Pd to take into account the different content of active metal in the catalysts.

H_2O_2 selectivity ($S_{\text{H}_2\text{O}_2}$) and specific conversion ($C_{\text{H}_2\text{O}_2}$) were calculated as follows:

$$S_{\text{H}_2\text{O}_2} = \frac{[\text{H}_2\text{O}_2]}{[\text{H}_2\text{O}_2] + [\text{H}_2\text{O}]} \times 100$$

$$C_{\text{H}_2\text{O}_2} = \frac{[\text{H}_2\text{O}_2] + [\text{H}_2\text{O}]}{\dot{n}_{\text{H}_2} \times t} \times V^L \times 100$$

where $[\text{H}_2\text{O}_2]$ and $[\text{H}_2\text{O}]$ are the concentration of peroxide and water, respectively, V^L is the liquid volume in the reactor and \dot{n}_{H_2} is the inlet molar flow of H_2 , t is time. Prior to the introduction of the catalyst, water content of the liquid phase was measured and deducted from the subsequent analysis.

3. Results and discussion

3.1. Porosity analysis

Being rather different in composition, the calcined supports exhibit a rather wide range of BET surface area, from 30 to over 100 m^2/g . The average pore diameter range is also quite wide, from about 5 up to 28 nm, as well as the total pore volume that affected the number of steps necessary for the impregnation of the Pd precursor. As expected, samples with high surface area present low pore volume and pore diameter (see Table 2).

3.2. XRD

Fig. 1 shows the XRD spectra of catalysts prepared using MEL supports. All the supports formed a solid solution between zirconia and the promoter present in the powder. Indeed, both Pd2 and Pd3 show peaks of tetragonal $\text{Zr}_{0.84}\text{Ce}_{0.16}\text{O}_2$ as main phase. Pd2 also shows some low peaks due to residual amounts of ZrO_2 , which are not at all present in the pattern of Pd3. Pd6 shows the formation of tetragonal $\text{Zr}_{0.9}\text{Y}_{0.1}\text{O}_{1.95}$, while the Pd7 sample exhibits overlapping peaks originated by the formation of cubic zirconium lanthanum oxide ($\text{Zr}_{0.9}\text{La}_{0.1}\text{O}_{1.95}$) and tetragonal zirconium cerium oxide ($\text{Zr}_{0.9}\text{Ce}_{0.1}\text{O}_2$).

The patterns of the remaining samples are reported in Fig. 3, where 2 references patterns are also included. CeO_2 – ZrO_2 mix is a sample of ceria and zirconia that were mixed and crushed together, but not calcined, while the pattern on top of the figure is representative of a solid solution between ceria and zirconia. The spectra in Fig. 3 shows that these samples are more crystalline compared to those prepared with MEL supports. Indeed the peaks in Fig. 2 are broader and less intense, probably due both a loss of crystallinity and a decrease of the particle size of the supports as already reported for this kind of materials [23–25]. As expected the samples prepared by mixing, crushing and calcining different amounts of ceria and zirconia, did not form a solid solution, but rather maintained the character of distinct phases. However, both the patterns of Pd4 and Pd5 show a marked reduction of the peaks due to pure

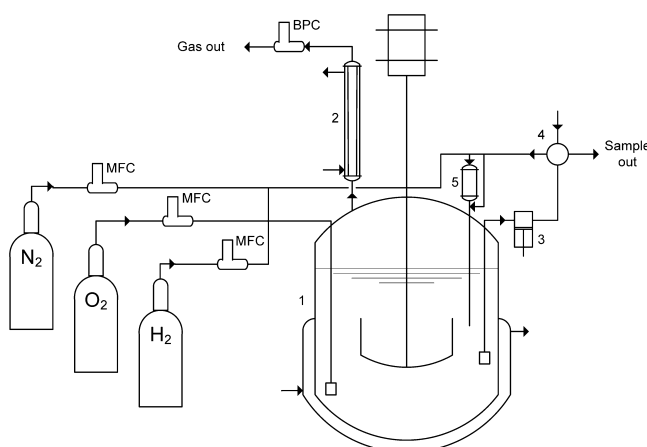


Fig. 1. Schematic of the experimental apparatus: 1—reactor; 2—condenser; 3—high pressure pump; 4—sampling valve; 5—catalyst chamber; MFC—mass flow controller; BPC—back pressure controller.

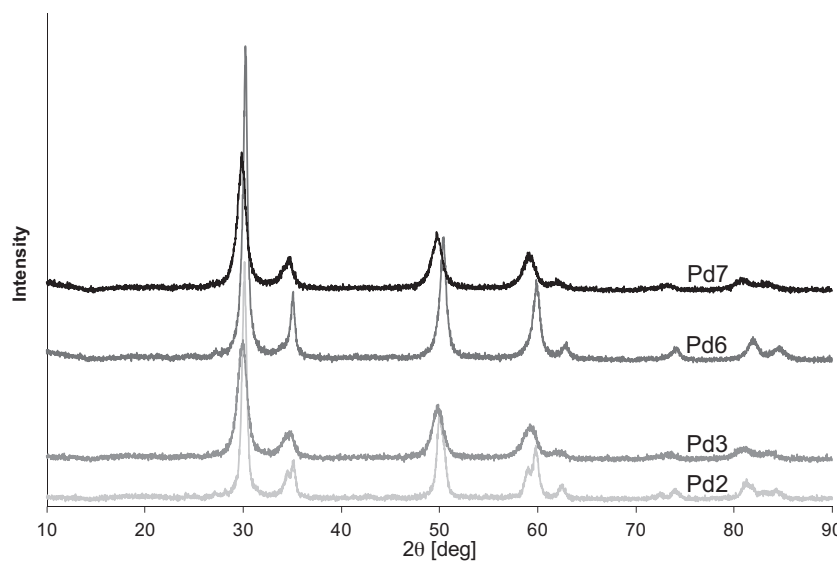


Fig. 2. XRD patterns of the Pd samples supported on MEL Chemicals powders. Pd2: $\text{ZrO}_2/\text{CeO}_2$ 82.5/17.5, Pd3: Ce doped ZrO_2 , Pd6: $\text{ZrO}_2/\text{Y}_2\text{O}_3$ 92/8, Pd7: $\text{ZrO}_2/\text{CeO}_2/\text{La}_2\text{O}_3$ 77.5/17.5/5.

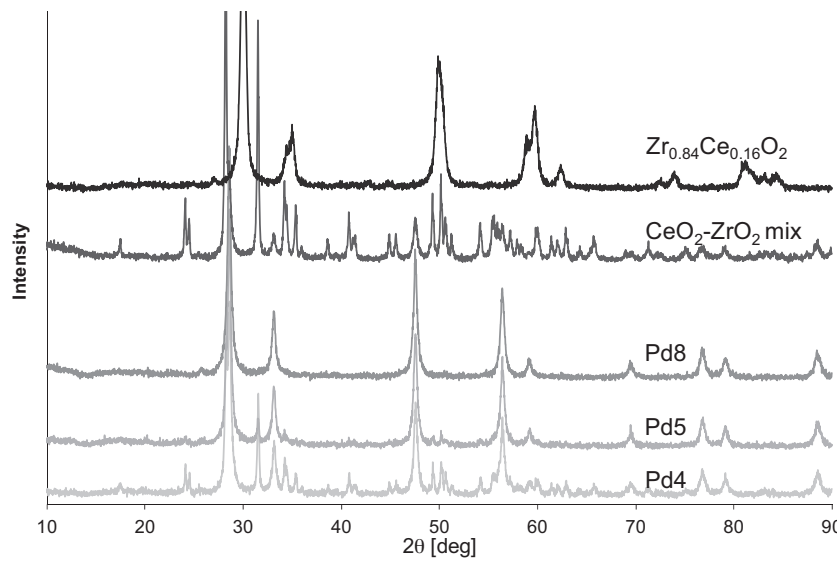


Fig. 3. XRD patterns of the Pd samples supported on ceria-zirconia mixtures. Pd4: $\text{CeO}_2/\text{ZrO}_2$ 17/83. Pd5: $\text{CeO}_2/\text{ZrO}_2$ 50/50, Pd8: CeO_2 . For comparison, the pattern of a non calcined $\text{CeO}_2/\text{ZrO}_2$ 17/83 is also reported, as well as the pattern of a solid solution of ceria and zirconia.

ZrO_2 . This can be noted mainly by observing the peak at 31.54° and the pair of overlapping peaks at 24.1 and 24.5°, which becomes much smaller in the spectra of Pd4 and Pd5. As a matter of fact, the formation of some $\text{Ce}_{0.75}\text{Zr}_{0.25}\text{O}_2$ is also detected in both these samples. The main peaks, though, are due to the presence of cubic ceria and monoclinic ZrO_2 .

No peaks of Pd were detected, due to both the small particles size and the low amount of metal loaded on the samples.

3.3. CO chemisorption

As highlighted in Table 2, the support physical features considerably affect the metal dispersion and the average particle size. There seem to be a trend according to which the dispersion is both directly dependent on the pore diameter and inversely proportional to the surface area of the support. In particular, it appears quite clear that supports with larger pore diameter allowed the formation of smaller particles, thus favoring the metal dispersion. Conversely, on supports with small pores, the Pd particles are less likely to grow

outside the pores, this resulting in bigger particles. In general, the dispersion of all the samples is very high, ranging from 50 up to almost 100%.

3.4. Atomic absorption spectroscopy

The results of the measurement of the metal loading are reported in Table 2 and show that for all the samples the actual loading is rather close to the nominal, desired one; this being 0.3 wt.% for the samples supported on MEL Chemicals powders and 0.6 wt.% for the remaining samples. The measurements were repeated 5 times on each sample and the relative standard deviation was always smaller than 2%.

3.5. TPR profiles

All the prepared sample show a clear negative peak centered around 70 °C. Another smaller peak (barely detectable in some

cases) is centered at around 48 °C. Both the peaks slightly shift their position between 68 and 76 °C and 46 and 49 °C.

For the samples supported on MEL supports (Fig. 4), other palladium reduction peaks are detected at varying temperatures. Indeed, Pd2 shows a peak between 300 and 400 °C; Pd3 shows a peak starting at about 170 °C and overlapping with another very wide one at 400 °C, the latter likely due to the support. Pd6 shows a reduction peak centered at 307 °C, while sample 7 exhibits a peak at 93 °C. All the peaks below 80 °C are due to the decomposition of Pd β-hydride [26–28]. In fact, PdO can be reduced at temperatures as low as –15 °C, leading to the formation of β-hydride that later decomposes releasing H₂. The reduction of PdO occurs in before the analysis starts, when H₂ is dosed at room temperature until the TCD base line stabilizes. When the TPR run starts, the freshly formed hydride decomposes, originating the negative peaks at around 70 °C.

The peaks between 80 and 350 °C are due to Pd(II) non reducible at room temperature, as also reported in [29–31]. In particular, according to the cited studies, the high temperature reduction peaks can be assigned to two dimensional PdO that can be formed on the surface in case of low Pd content. It is also reported that this kind of PdO structure is formed in presence of highly dispersed metal, due to small crystallite size. This is in agreement with the high dispersion values detected and the consequent low particles size of our samples. Interestingly, no Pd reduction peaks are detected for the samples at higher Pd load (Fig. 5). Only a more pronounced negative peak at 75 °C is detected. Other peaks are detected at much higher temperature, but they are very small and they seem to correspond to those obtained in the reduction of the bare supports. It appears that the loaded Pd is suppressing the reduction of the support.

3.6. Experimental results

All experiments were carried out in a semibatch reactor, where the reagents were continuously bubbled through the static liquid phase. Prior to the experimental campaign, the reactor setup was tested for eventual external mass transfer limitations. Given that the gas to liquid mass transfer is independent of the specific catalyst, increasing amounts of a commercial 5% Pd on carbon catalyst (Degussa) were tested in similar reaction conditions. Since a high H₂ conversion was the aim of these experiments, a catalyst with a higher Pd content compared to our synthesized materials was deliberately chosen. A linear conversion of H₂ (the limiting reagent) was observed up to 80% (Supplementary material, Fig. 1), confirming that the reaction was not affected by gas to liquid transport limitations. Hence, all experiments herein reported were carried out at H₂ conversion below 80%. Experimental results are reported in Fig. 6 in terms of peroxide specific concentration, selectivity and conversion as a function of time.

In all experiments, hydrogen peroxide concentration leaned towards a steady state value. At the same time, the selectivity dropped, meaning that the water concentration (not shown) steadily increased. This is expected, since hydrogen peroxide is a reaction intermediate and water is the final product (Scheme 1); in a semibatch apparatus the accumulation of peroxide leads to an increase of the hydrogenation and disproportionation rates, so that its concentration will reach an equilibrium value, at the same time dropping the selectivity. This evolution is particularly evident with the catalysts showing the highest H₂ conversion. Interestingly, the conversion decreased with the time on stream (Fig. 6C), which is in apparent contradiction with the increasing peroxide (and water) concentrations. This effect is due to the solubility of H₂ in the liquid phase. As soon as the catalyst was introduced, H₂ started to react, creating a sink of H₂ that was refilled by the inlet gas flow. The gas phase behaved like a continuous stream reactor, where the composition at the outlet is equal to the composition

inside the reactor. Because of the reactions, the composition of the outlet gas (and hence inside the reactor) dropped, causing a drop in the liquid composition, which in return impaired the reaction rates and hence the conversion. In other words, because of the reactions, the liquid phase goes through a transient from a higher to a lower H₂ (and O₂) content, that caused a decrease in the H₂ conversion. Moreover, the decreased composition in the liquid phase caused a buffer (reservoir) of H₂ in the methanol. This quantity of H₂ was available to the reactions but is not included in the definition of conversion given in the previous section. This contributed to the very high conversion values observed at low contact time (<10 min). The effect is only noticeable at low time on stream (<10 min), as the H₂ buffer is soon consumed. Including the effect of the H₂ reservoir is in principle possible, but it would require the precise knowledge of the vapor–liquid equilibrium of the complex system H₂–O₂–N₂–methanol and numerical modelling of the reactor, which goes beyond the scopes of the present work. Nonetheless, the reported conversion values are significant to quantitatively evaluate the activity of the synthesized catalysts.

A 1 wt.% Pd on carbon commercial catalyst was tested as a benchmark. Apparently, all our synthesized catalysts had a lower conversion. However, the Pd content of the commercial was much higher, so that the conversion compare well with our original catalysts when normalized. Furthermore, most our catalysts reached a much higher peroxide specific concentration and selectivity, with values up to 4 times larger. The catalysts supported on MEL supports (Pd2, Pd6, Pd7) showed the highest H₂ conversion. In particular, the catalysts Pd2, Pd6 and Pd7 had the same conversion throughout the experiment, reaching values around 20% after 5 h of reaction, whereas the other catalysts showed 9% conversion. Note that the catalysts supported on MEL supports had half the Pd content of the others (Table 2), so that their relative activity is actually much higher than the other catalysts. These conversion values are apparently rather low. As a comparison, Menegazzo et al. [14] found values between 45% and 54% at 5 h reaction, depending on the calcination temperature of a 1.5 wt.% SiO₂/Pd catalyst; the same research group reported values between 40% and 90% with Pd catalysts (2.5 wt.%) supported on Zirconia and Ceria [15] (5 h reaction). However, in the present study the experimental conditions (in particular the ratio between the H₂ flow rate and the catalyst quantity) were chosen so that the conversion never exceeded 30% for high time on stream to avoid any possible mass transfer limitation. Moreover, the conversion strongly depends on the total active metal used in the experiments, so that values are more significant when normalized. Hence, in our study specific conversions in the range of 46–100 $\left(\text{mol}_{\text{H}_2}^{\text{consumed}} \times \left(\text{mol}_{\text{H}_2}^{\text{supplied}} \right)^{-1} \times (\text{mmol}_{\text{Pd}})^{-1} \right)$

were obtained at 5 h time on stream, whereas in the mentioned studies [14,15] the specific conversion was between 24 and 40 $\left(\text{mol}_{\text{H}_2}^{\text{consumed}} \times \left(\text{mol}_{\text{H}_2}^{\text{supplied}} \right)^{-1} \times (\text{mmol}_{\text{Pd}})^{-1} \right)$. The

same catalysts Pd2, Pd3, Pd6 and Pd7 also showed the highest H₂O₂ specific concentration (Fig. 6A), with values of 3.5 and 8.5 ($\text{M}_{\text{H}_2\text{O}_2} \text{ mmol}_{\text{Pd}}^{-1}$) for the groups Pd2, Pd3 and Pd6, Pd7, respectively. Lower values are normally reported in the literature. For instance, Abate et al. [12] obtained peroxide specific concentrations in the range 2.1–5.2 ($\text{M}_{\text{H}_2\text{O}_2} \text{ mmol}_{\text{Pd}}^{-1}$) at 4 h contact time in a 6.5 bar semibatch apparatus; Menegazzo et al. [14,15] obtained values between 0.2 and 4.2 ($\text{M}_{\text{H}_2\text{O}_2} \text{ mmol}_{\text{Pd}}^{-1}$) in atmospheric conditions at 5 h contact time, depending on the catalyst. However, a higher peroxide concentration value is expected in our system. Indeed, due to the higher pressure (50 bar), a higher reagent concentration was reached, allowing achieving a higher production

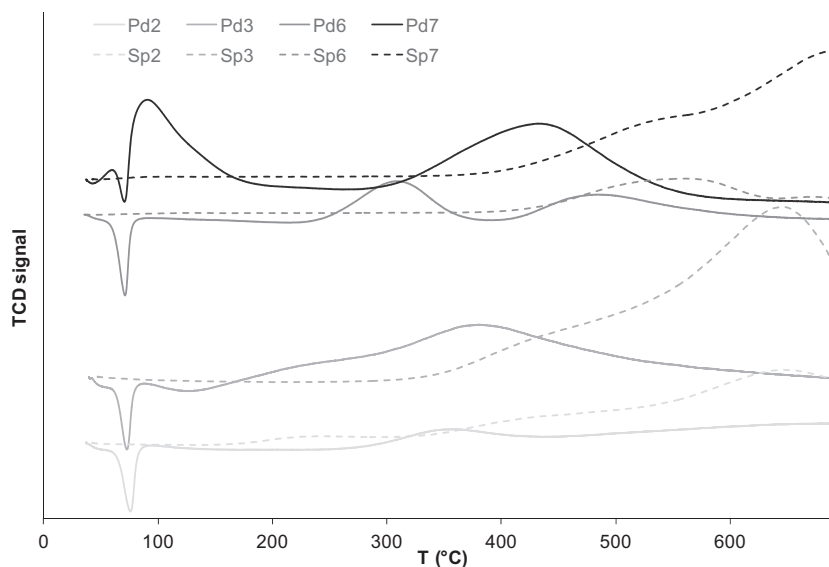


Fig. 4. TPR curves of the fresh samples and of the supports for the 0.3% Pd samples.

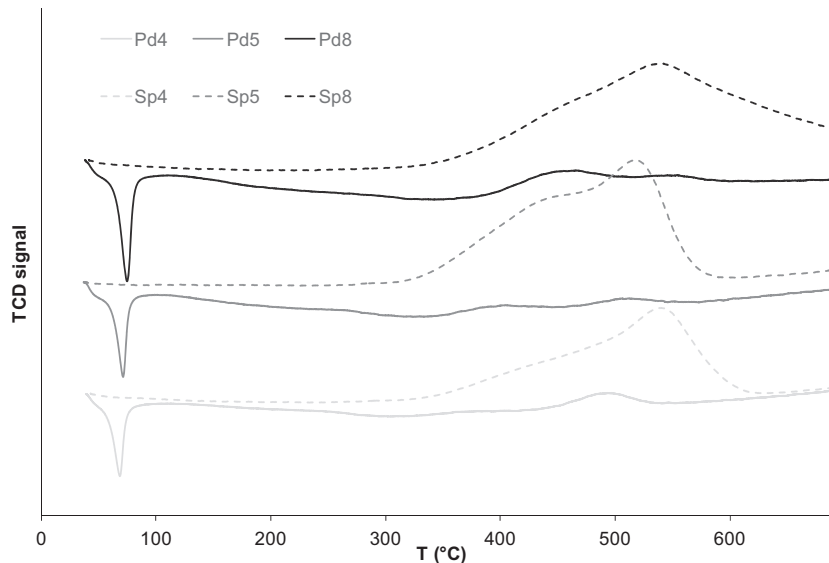


Fig. 5. TPR curves of the fresh samples and of the supports for the 0.6% Pd samples.

rate. Interestingly, the catalysts with the highest specific peroxide concentration showed also the highest selectivity (Fig. 6B). Nonetheless, the selectivity was quite low compared to the values obtained in the literature in similar apparatus [12,14,15,32]. It is worth noticing that in all literature studies promoters and stabilizers (such as bromine and/or acids) were introduced in the reaction slurry to enhance selectivity and productivity. No such chemicals were used in this study, in order to isolate the effect of the catalyst properties on the selectivity.

In the following, the experimental results are discussed in relation to the catalyst' properties. Interestingly, the sample with the lowest Pd content (Table 2) showed the highest selectivity and specific peroxide concentrations. More specifically, this relates to the interaction between the active metal and the support, where smaller pore diameters allowed the formation of larger Pd particles. In order to quantify this effect, in Fig. 7 the selectivity and the specific peroxide concentration are reported as a function of the Pd particle size. Since the measurements varied with time (Fig. 6), comparisons were carried out at 1 h and 5 h time on stream.

Selectivity and peroxide concentration evolutions were independent on the contact time, suggesting that the choice of the reaction time for the comparison can be arbitrary. The larger the Pd particle, the higher the concentration and the selectivity toward the desired product obtained. This suggests that larger particles of the active metal suppressed the formation of water, favoring the production of the peroxide. It has been proposed [14,16] that O₂ adsorbs associatively on less energetic Pd particles, thus favoring H₂O₂ formation. On the contrary, highly unsaturated sites, such as Pd atoms at a corner or an edge cleave the O–O bond, leading to the non-selective production of H₂O. The morphological properties of the catalysts presented in this work support this hypothesis, where large and thus less energetic particles favored the direct synthesis of H₂O₂. Fig. 7 highlights the superiority of the samples supported on solid solutions of ZrO₂ with its promoters. Indeed, the samples that perform better are those that presented a Zr_xM_{1-x}O₂ structure (M = La, Y, Ce). The Pd2 sample seems to be an exception, since it exhibits activity and selectivity that are generally more in line with the performance of the samples that did not form a solid solution.

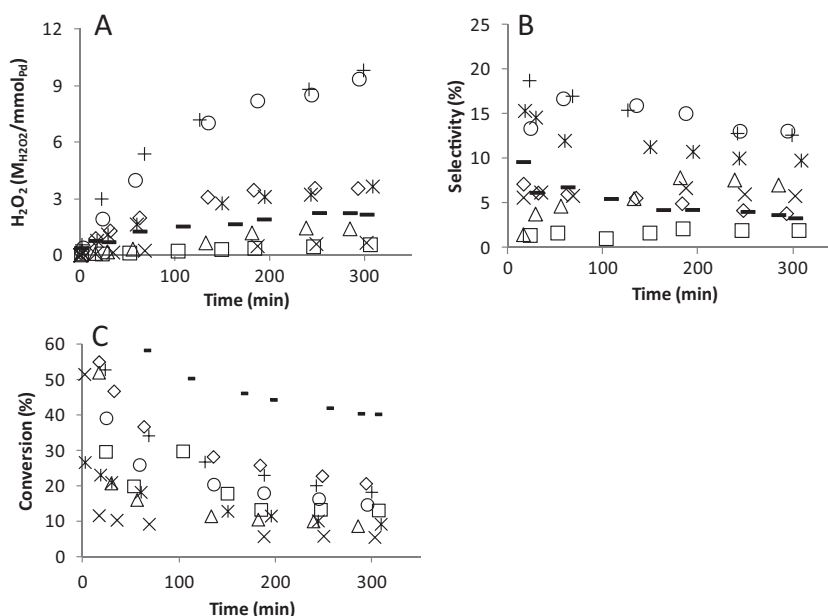


Fig. 6. Experimental results in terms of specific H_2O_2 concentration (A), selectivity (B) and conversion (C): \diamond , Pd2; $*$, Pd3; \times , Pd4; \square , Pd5; \circ , Pd6; $+$, Pd7; \triangle , Pd8; –, Pd/C commercial.

However, its H_2O_2 productivity after 1 h is perfectly aligned with the general trend. The reason for the lower performance of Pd2 might be the presence of residual amounts of ZrO_2 in its support structure, as evidenced by the XRD pattern. This fact can also be correlated with the redox behavior of the samples. Indeed, Pd2 shows a much smaller Pd reduction peak than any other sample that forms a solid $\text{Zr}_x\text{M}_{1-x}\text{O}_2$ solution (see Fig. 4). Conversely, Pd2 shows a TPR profile that is closer to that of the samples supported on mechanical mixtures of ceria and zirconia, which in turn show much lower activity and selectivity. It is well known that metallic catalysts supported on homogenous solid solution of ZrO_2 with promoters such Ce, Y and La, become more reducible than when supported on pure ZrO_2 [21,22]. The redox properties of the metal/support system are very important in determining the final performance of the catalyst. In particular, more reducible systems can achieve higher selectivity and production of H_2O_2 [9,17]. Furthermore, the promoters also stabilize the physical properties, preserving a higher

surface area upon exposure to high temperature. Observing the supports features reported in Table 2, it is clear that Ce did not have an as good stabilizing effect for the Pd2 sample as for the Pd3 one. Indeed, the Pd2 surface area is only 52 vs 93 m^2/g for Pd3. Accordingly, the average pore diameter and the total pore volume are also different. Looking closer, one can note that the better performing samples (Pd3, Pd6 and Pd7) present a very low average pore diameter (5–7 nm). On the contrary, the remaining samples, whose performance are lower, present an average pore diameter in the range of 16–30 nm. The same observation stands for the total pore volume, with the better performing catalysts showing a value that is about half or less than the remaining samples. This is reflected on the size of the Pd particles, with the exception of Pd2.

We conclude that both the support physical features and the global redox properties strongly affect the behavior of the catalyst, with bigger metal particles and higher reducibility favoring the production of H_2O_2 .

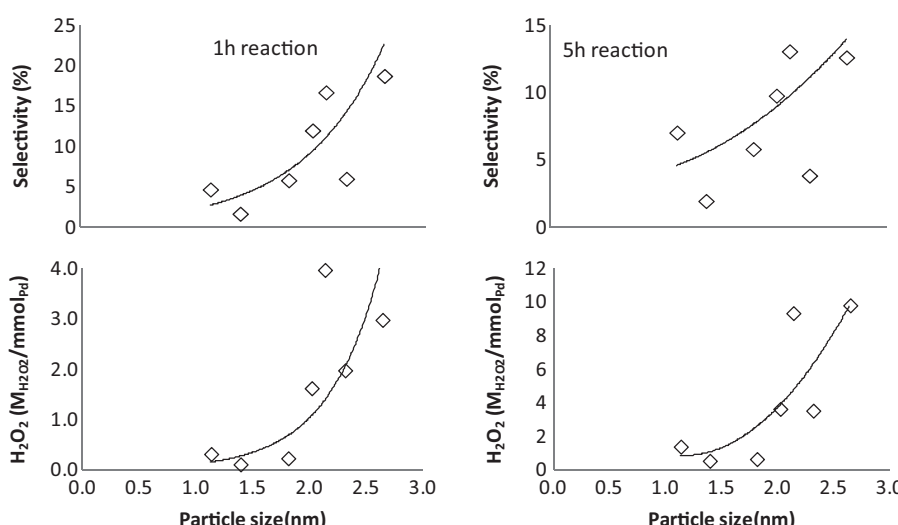


Fig. 7. Selectivity (top) and specific peroxide concentration (bottom) after 1 h (left) and 5 h (right) time on stream as a function of the Pd particle size of the catalyst.

4. Conclusions

Novel catalysts for the direct synthesis of hydrogen peroxide were prepared supporting Pd on mixed oxides (ZrO_2 and CeO_2) and rare earth elements (Y_2O_3 and La_2O_3). These materials were chosen because of their capability of increasing both the metal dispersion and the O_2 mobility (which favors the active metal activity). Furthermore, their properties (surface area, pore volume, particle size, homogeneity, etc) are easily tunable changing the preparation procedures. XRD analysis showed the formation of $Zr_xM_{1-x}O_2$ ($M = La, Y, Ce$) solid solutions for the supports supplied by MEL Chemicals, but the persistence of separate ceria and zirconia phases for the supports prepared by mixing and calcining different amounts of ceria and zirconia. All the samples achieved very high dispersion (50–99%) resulting from a very small average particle size (1–2.6 nm). Through TPR it was shown that the supports features affect the reducibility of the metal–support system and this result in rather different catalytic performance. More easily reducible samples exhibited higher performance. Hydrogen peroxide direct synthesis was performed in a high pressure semibatch reactor in the absence of promoters and stabilizers (acid and hides). H_2 conversion and peroxide concentration obtained were higher than usually reported in the literature using similar apparatus. Specific conversion and selectivity up to 4 times higher compared to a commercial Pd/C catalyst were achieved, and up to double the values reported in literature in works where enhancers were used. The synthesis reaction was run in a broad range of product concentration, with the peroxide leaning towards a steady state value due to the subsequent reactions. Larger Pd particles were obtained upon supports with smaller pore diameters. In turns, the larger Pd particles were more selective toward the peroxide, suggesting that highly unsaturated sites, such as Pd atoms at a corner or an edge largely present on small particles, cleave the O–O bond, leading to water. Furthermore, supports with higher reducibility favored the production of H_2O_2 , probably due to an easier reduction of the active metal, essential to achieve high selectivity. These observations lead to conclude that highly reducible supports giving larger metal particles are most desirable in the preparation of catalysts for the H_2O_2 direct synthesis.

Acknowledgments

This work is part of the activities Process Chemistry Centre (PCC) financed by the Åbo Akademi University (ÅA). Dr. Pierdomenico Biasi gratefully acknowledges the Kempe Foundations (Kempe Stiftelsen) for financial support. In Sweden, also the Bio4Energy program is acknowledged.

Appendix A. Supplementary data

Supplementary data associated with this article can be found, in the online version, at <http://dx.doi.org/10.1016/j.cattod.2014.12.033>.

References

- [1] C. Samanta, Direct synthesis of hydrogen peroxide from hydrogen and oxygen: an overview of recent developments in the process, *Appl. Catal., A: Gen.* 350 (2008) 133–149.
- [2] J. García-Serna, T. Moreno, P. Biasi, M.J. Cocero, J. Mikkola, T.O. Salmi, Engineering in direct synthesis of hydrogen peroxide: targets, reactors and guidelines for operational conditions, *Green Chem.* 16 (2014) 2320–2343.
- [3] G. Centi, S. Perathoner, S. Abate, Direct synthesis of hydrogen peroxide: recent advances, in: *Modern Heterogeneous Oxidation Catalysis*, Wiley-VCH Verlag GmbH & Co. KGaA, Weinheim, Germany, 2009, pp. 253–287.
- [4] J.M. Campos-Martin, G. Blanco-Brieva, J.L.G. Fierro, Hydrogen peroxide synthesis: an outlook beyond the anthraquinone process, *Angew. Chem. Int. Ed.* 45 (2006) 6962–6984.
- [5] N. Gemo, P. Biasi, P. Canu, T.O. Salmi, Mass transfer and kinetics of H_2O_2 direct synthesis in a batch slurry reactor, *Chem. Eng. J.* 207–208 (2012) 539–551.
- [6] I. Huerta, J. García-Serna, M.J. Cocero, Hydrogenation and decomposition kinetic study of H_2O_2 over Pd/C catalyst in an aqueous medium at high CO_2 pressure, *J. Supercrit. Fluids* 74 (2013) 80–88.
- [7] Y. Voloshin, A. Lawal, Kinetics of hydrogen peroxide reduction by hydrogen in a microreactor, *Appl. Catal., A: Gen.* 353 (2009) 9–16.
- [8] E.N. Ntainjua, J.K. Edwards, A.F. Carley, J.A. Lopez-Sánchez, J.A. Moulijn, A.A. Herzing, C.J. Kiely, G.J. Hutchings, The role of the support in achieving high selectivity in the direct formation of hydrogen peroxide, *Green Chem.* 10 (2008) 1162–1169.
- [9] C. Burato, S. Campestrini, Y. Han, P. Canton, P. Centomo, P. Canu, B. Corain, Chemoselective and re-usable heterogeneous catalysts for the direct synthesis of hydrogen peroxide in the liquid phase under non-explosive conditions and in the absence of chemoselectivity enhancers, *Appl. Catal., A: Gen.* 358 (2009) 224–231.
- [10] G. Blanco-Brieva, E. Cano-Serrano, J. Campos-Martin, J.L.G. Fierro, Direct synthesis of hydrogen peroxide solution with palladium-loaded sulfonic acid polystyrene resins, *Chem. Commun.* 0 (2004) 1184–1185.
- [11] S. Abate, S. Perathoner, G. Centi, Performances of Pd nanoparticles on different supports in the direct synthesis of H_2O_2 in CO_2 -expanded methanol, *Top. Catal.* 54 (2011) 718–728.
- [12] S. Abate, P. Lanzafame, S. Perathoner, G. Centi, SBA-15 as a support for palladium in the direct synthesis of H_2O_2 from H_2 and O_2 , *Catal. Today* 169 (2011) 167–174.
- [13] E. Ghedini, F. Menegazzo, M. Signoretto, M. Manzoli, F. Pinna, G. Strukul, Mesoporous silica as supports for Pd-catalyzed H_2O_2 direct synthesis: effect of the textural properties of the support on the activity and selectivity, *J. Catal.* 273 (2010) 266–273.
- [14] F. Menegazzo, M. Signoretto, G. Frison, F. Pinna, G. Strukul, M. Manzoli, F. Bocuzzi, When high metal dispersion has a detrimental effect: hydrogen peroxide direct synthesis under very mild and nonexplosive conditions catalyzed by Pd supported on silica, *J. Catal.* 290 (2012) 143–150.
- [15] F. Menegazzo, P. Burti, M. Signoretto, M. Manzoli, S. Vankova, F. Bocuzzi, F. Pinna, G. Strukul, Effect of the addition of Au in zirconia and ceria supported Pd catalysts for the direct synthesis of hydrogen peroxide, *J. Catal.* 257 (2008) 369–381.
- [16] S. Abate, G. Centi, S. Melada, S. Perathoner, F. Pinna, G. Strukul, Preparation, performances and reaction mechanism for the synthesis of H_2O_2 from H_2 and O_2 based on palladium membranes, *Catal. Today* 104 (2005) 323–328.
- [17] Q. Liu, K. Gath, J. Bauer, R. Schaal, J. Lunsford, The active phase in the direct synthesis of H_2O_2 from H_2 and O_2 over Pd/SiO₂ catalyst in a H_2SO_4 /ethanol system, *Catal. Lett.* 132 (2009) 342–348.
- [18] S. Eriksson, S. Rojas, M. Boutonnet, J.L.G. Fierro, Effect of Ce-doping on Rh/ ZrO_2 catalysts for partial oxidation of methane, *Appl. Catal., A: Gen.* 326 (2007) 8–16.
- [19] S. Boullosa-Eiras, T. Zhao, D. Chen, A. Holmen, Effect of the preparation methods and alumina nanoparticles on the catalytic performance of Rh/ $Zr_xCe_{1-x}O_2$ –Al₂O₃ in methane partial oxidation, *Catal. Today* 171 (2011) 104–115.
- [20] M. Pudukudy, Z. Yaakob, Catalytic aspects of ceria zirconia solid solution: Part-II: An overview on recent developments in the heterogeneous catalytic applications of metal loaded ceria–zirconia solid solution, *Pharma Chem.* 6 (2014) 224.
- [21] M. Pudukudy, Z. Yaakob, Catalytic aspects of ceria–zirconia solid solution: Part-I: An update in the synthesis, properties and chemical reactions of ceria zirconia solid solution, *Pharma Chem.* 6 (2014) 188.
- [22] Y. Han, J. Zhu, Surface science studies on the zirconia-based model catalysts, *Top. Catal.* 56 (2013) 1525–1541.
- [23] R. Pérez-Hernández, L.C. Longoria, J. Palacios, M.M. Aguilera, V. Rodríguez, Oxidative steam reforming of methanol for hydrogen production over Cu/ CeO_2 – ZrO_2 catalysts, *Energy Mater.* 3 (2008) 152–157.
- [24] R. Pérez-Hernández, A. Gómez-Cortés, J. Arenas-Alatorre, S. Rojas, R. Mariscal, J.L.G. Fierro, G. Díaz, SCR of NO by CH_4 on Pt/ ZrO_2 –TiO₂ sol-gel catalysts, *Catal. Today* 107–108 (2005) 149–156.
- [25] R. Pérez-Hernández, F. Aguilar, A. Gómez-Cortés, G. Díaz, NO reduction with CH_4 or CO on Pt/ ZrO_2 –CeO₂ catalysts, *Catal. Today* 107–108 (2005) 175–180.
- [26] Z. Pál, P.G. Menon, *Hydrogen Effects in Catalysis: Fundamental and Practical Applications*, Marcel Dekker, New York, U.S.A., 1988.
- [27] Z. Karpinski, Catalysis by supported, unsupported, and electron-deficient palladium, *Adv. Catal.* 37 (1990) 45–100.
- [28] P.C. Aben, Palladium areas in supported catalysts: determination of palladium surface areas in supported catalysts by means of hydrogen chemisorption, *J. Catal.* 10 (1968) 224–229.
- [29] S. Melada, R. Riada, F. Menegazzo, F. Pinna, G. Strukul, Direct synthesis of hydrogen peroxide on zirconia-supported catalysts under mild conditions, *J. Catal.* 239 (2006) 422–430.
- [30] N.S. Babu, N. Lingaiah, R. Gopinath, P.S. Sankar Reddy, P.S. Sai Prasad, Characterization and reactivity of alumina-supported Pd catalysts for the room-temperature hydrodechlorination of chlorobenzene, *J. Phys. Chem. C* 111 (2007) 6447–6453.
- [31] A. Barrera, M. Viniegra, S. Fuentes, G. Díaz, The role of lanthana loading on the catalytic properties of Pd/Al₂O₃–La₂O₃ in the NO reduction with H_2 , *Appl. Catal., B: Environ.* 56 (2005) 279–288.
- [32] T. Moreno, J. García-Serna, P. Plucinski, M.J. Sánchez-Montero, M.J. Cocero, Direct synthesis of H_2O_2 in methanol at low pressures over Pd/C catalyst: semi-continuous process, *Appl. Catal., A: Gen.* 386 (2010) 28–33.